

C.K.Y. Yiu¹, F.R. Tay^{1*}, N.M. King¹,
D.H. Pashley², S.K. Sidhu³, J.C.L. Neo⁴,
M. Toledano⁵, and S.L. Wong⁶

¹Paediatric Dentistry and Orthodontics, Faculty of Dentistry, University of Hong Kong, Prince Philip Dental Hospital, 34 Hospital Road, Hong Kong SAR, China; ²Department of Oral Biology and Maxillofacial Pathology, Medical College of Georgia, Augusta, GA, USA; ³Department of Restorative Dentistry, University of Newcastle, Newcastle upon Tyne, UK; ⁴Department of Restorative Dentistry, National University of Singapore, Singapore; ⁵Department of Dental Materials, University of Granada, Spain; and ⁶Electron Microscopy Unit, University of Hong Kong, Hong Kong SAR, China; *corresponding author, kfctay@hknet.com

J Dent Res 83(4):283-289, 2004

ABSTRACT

Glass-ionomer cements (GICs) are regarded as aqueous gels made up of polyalkenoic acid salts containing ion-leachable glass fillers. The consequence of water permeation across the GIC-dentin interface is unknown. This study used SEM, field-emission/environmental SEM (FE-ESEM), and TEM to examine the ultrastructure of GIC-bonded moist dentin. Dentin surfaces bonded with 6 auto-cured GICs were examined along the fractured GIC-dentin interfaces. Additional specimens fractured 3 mm away from the interfaces were used as controls. SEM revealed spherical bodies along GIC-dentin interfaces that resembled hollow eggshells. FE-SEM depicted similar bodies with additional solid cores. Energy-dispersive x-ray analysis and TEM showed that the spherical bodies consisted of a silicon-rich GIC phase that was absent from the air-voids in the controls. The GIC inclusions near dentin surfaces result from a continuation of the GI reaction, within air-voids of the original polyalkenoate matrix, that occurred upon water diffusion from moist dentin.

KEY WORDS: glass ionomer, spherical bodies, water, diffusion.

Interaction of Glass-ionomer Cements with Moist Dentin

INTRODUCTION

Glass-ionomer cements (GICs) exhibit several clinical advantages compared with other restorative materials. They include physicochemical bonding to tooth structures (Glasspoole *et al.*, 2002), long-term fluoride release, and low coefficients of thermal expansion (Nassan and Watson, 1998). However, their low mechanical strength compromises their use in high-stress-bearing restorations (Kerby and Knobloch, 1992). The acid-base setting reaction in GICs is initiated by the depletion of metallic ions from the fluoro-aluminosilicate glass (FASG) fillers by polyalkenoic acid, leaving siliceous hydrogel layers on the surface of the glass particles (Hatton and Brook, 1992; Nicholson, 1998). Cross-linking of these ions with polyalkenoic acid results in the formation of a primary polysalt matrix within the set cement (Maeda *et al.*, 1999). A secondary reaction that leads to the deposition of a silicate phase contributes to the gradual increase in compressive strength with time (Wasson and Nicholson, 1993; Matsuya *et al.*, 1996).

To date, both ultrastructural and analytical evidence is available on the existence of an intermediate layer along the GIC-dentin/enamel interfaces that is caused by ion exchange between the material and tooth substrate (Geiger and Weiner, 1993; Ngo *et al.*, 1997; Ferrari and Davidson, 1997; Sennou *et al.*, 1999; Tay *et al.*, 2001a; Yip *et al.*, 2001). Water permeation from dentin into GICs (Watson *et al.*, 1991, 1998) or resin-modified GICs (Sidhu and Watson, 1998) has been observed by dynamic laser confocal microscopy. This phenomenon of localized water sorption has not been previously observed in GIC-bonded dentin. The consequence of such water permeation across the GIC-dentin interface is unknown.

This study used scanning electron microscopy (SEM), field-emission/environmental SEM (FE-ESEM), and transmission electron microscopy (TEM) to examine the regional differences in the ultrastructure of GIC bonded onto moist human dentin. Dentin surfaces bonded with 6 auto-cured GICs were examined along the fractured GIC-dentin interfaces. Additional GIC specimens were fractured 3 mm away from the interfaces, and fractured unbonded GIC samples were used as controls. The null hypothesis tested was that there is no difference among the ultrastructural features of GICs fractured at different locations from the bonded dentin, and fractured unbonded GICs.

MATERIALS & METHODS

Bonding was performed on the occlusal surfaces of deep coronal dentin of extracted human third molars. The teeth were collected after the patients' informed consent had been obtained under a protocol reviewed and approved by the institutional review board at the Medical College of Georgia, Augusta, USA. The teeth were stored in 0.9% NaCl at 4°C and were used within 1 mo of extraction. The occlusal enamel was removed by means of a slow-speed saw (Isomet, Buehler Ltd., Lake Bluff, IL, USA) under water cooling, while the roots of these teeth were left intact.

Experimental Design

Dentin surfaces were abraded with 180-grit silicon carbide paper and further treated with polyacrylic acid (Cavity Conditioner; GC Corp., Tokyo, Japan) for 10 sec immediately before being bonded with the GICs. Five teeth were prepared for each of the 6 auto-cured GICs tested: Fuji IX GP and Fuji VII (GC Corp.), ChemFlex and Experimental batch K-136 (Dentsply DeTrey, Konstanz, Germany), Ketac-Molar Aplicap (3M ESPE, St. Paul, MN, USA), and Hy-Bond (Shofu, Kyoto, Japan). The GICs were dispensed/mixed and bonded according to the manufacturers' instructions, to form 6-mm-high cores over the surfaces of the moist dentin.

Additional GICs were mixed and applied to the surfaces of mylar strips, which were then allowed to cure without being bonded to tooth substrates.

After initial setting, both the bonded and unbonded GICs were covered with a thin layer of light-cured, oxygen-inhibition-layer-free, glaze resin (BisCover, Bisco Inc., Schaumburg, IL, USA), to prevent them from losing or gaining water *via* external sources. After storage at 37°C and 100% relative humidity for 48 hrs, the bonded specimens were cut occlusogingivally into 0.9 x 0.9 mm beams, following the method used for evaluation of microtensile bond strengths of GICs (Tay *et al.*, 2001a). With this technique, none of the specimens fractured during preparation into beams, confirming our previous experience. Similar beams were prepared from the unbonded GICs.

These beams were sealed in bottles at 100% humidity for 48 hrs before analyses. For SEM examination, 5 beams were randomly selected from the teeth bonded with each GIC, and fractured close to the GIC-dentin interface by three-point bending (razor blade at interface of end-supported beams). We fractured 5 additional bonded beams, at a location that was approximately 3 mm away from the bonded interfaces, by moving the supports. Both the dentin and GIC sides of these beams were air-dried, sputter-coated with gold/palladium, and examined with a SEM (Cambridge Stereoscan 440, Cambridge, UK) operating at 10 kV.

A similar number of beams from each group was used for FE-ESEM examination. The beams were fractured on-site, inserted immediately into the Peltier (cooling) stage of the microscope (Philips XL-30, Eindhoven, The Netherlands), and covered with water to avoid desiccation of the fractured GICs. They were examined at 15 kV, wet and without being coated, with the temperature of the Peltier stage fixed at 4°C and the vapor pressure of the specimen chamber varying between 5.4 and 5.9 Torr to generate a relative humidity of 96-99.9%. We used energy-dispersive x-ray (EDX) analysis to determine the composition of various structural phases identified by FE-ESEM along the fractured GIC-dentin interfaces.

To determine the extension of spherical bodies from bonded interfaces, we bonded 2 teeth with Fuji VII to form 6-mm-high cores over the surface of moist dentin, with the surface sealed with glaze resin. Bonded GIC-dentin slabs 2 mm wide were sectioned occluso-gingivally from the bonded teeth. They were polished under wet conditions with 1200-grit SiC paper, followed by 1 µm alpha alumina (Buehler Ltd.). These surfaces were briefly etched for 15 sec with 10% phosphoric acid (Bisco Inc.) to remove the smear layer and to bring the interfaces into relief. Two additional teeth were similarly bonded with Fuji VII, but without the surfaces being sealed with glaze resin. After setting of the GIC, these 2 teeth were immersed in distilled water for 10 min before storage at 100% relative humidity for 48 hrs. GIC-dentin slabs 2 mm wide

were similarly prepared and examined by FE-ESEM.

TEM examination was performed only on bonded GIC-dentin interfaces. Two beams were examined for each GIC. Intact beams (*i.e.*, without being fractured) were processed and resin-embedded according to the TEM protocol for GIC examination described by Tay *et al.* (2001a). Examination of 90-nm-thick sections was performed with a transmission electron microscope (Philips EM208S), operating at 80 kV.

RESULTS

Since the results were highly reproducible in all 6 GICs, only representative Figs. are shown. As expected, artifactual cracks were ubiquitously observed within the polyalkenoate matrix when the specimens were examined by conventional SEM. The corresponding dentin (Fig. 1A) and GIC (Fig. 1B) sides of a representative beam that was fractured along the GIC-dentin interface demonstrated the presence of numerous spherical bodies within the air-voids that were trapped inside the polyalkenoate matrix. The majority of the air-voids were filled with spherical bodies along the interface. These spherical bodies were easily discerned from the angular FASG fillers (Fig. 1C). Partially fractured spherical bodies revealed their hollow eggshell-like internal structure (Fig. 1D). Spherical bodies were absent from both the bonded specimens that were fractured at sites remote from the bonded interfaces (Fig. 1E), and in fractured unbonded GICs, where only air-voids could be identified. These spherical bodies ranged in size from 14 to 30 µm. Their wall thickness varied within the same spherical body and ranged from 0.4 to 3 µm.

Spherical bodies could also be seen under FE-ESEM when bonded GIC specimens were fractured along the GIC-dentin interface (Fig. 2A). In the absence of desiccation (Cowan *et al.*, 1996), no artifactual cracks were observed, and the spherical bodies were closely adapted to the GIC matrix. Dehydration cracks began to form in the polyalkenoate matrix when the pressure of the microscope chamber was reduced to 5.4 Torr (Fig. 2B). Fractured spherical bodies appeared solid under FE-ESEM examination (Fig. 2C). Similar to SEM observations, these spherical bodies were absent in unbonded GICs (Fig. 2D), as well as in bonded GICs that were fractured at sites remote from the bonded interfaces. Representative EDX spectra taken from the FASG fillers, polyalkenoate matrix, and spherical bodies are shown in Fig. 2E. As expected, Ca and P were predominantly absent from the FASG fillers. The Si content in the spherical bodies was approximately three times higher than that of the polyalkenoate matrices.

FE-ESEM examination of polished slabs revealed that, for resin-sealed GICs, spherical bodies were observed only along the GIC-dentin interfaces (Fig. 3A) and not along the surfaces of the resin-sealed GICs. The location of the spherical bodies that were farthest from the GIC-dentin interface was about 350 µm. No spherical bodies could be identified from the bonded GIC-enamel interfaces (not shown). For the unsealed GICs, spherical bodies could also be seen from the unsealed GIC surface (Fig. 3B). These bodies could be identified at about 180 µm from the GIC surface. Beyond this depth, only air-voids were exclusively observed.

TEM of GIC-dentin interfaces revealed the presence of a 2- to 3-µm-thick intermediate layer between the dentin and all of the GICs that were fractured during ultramicrotomy (Fig. 4A).

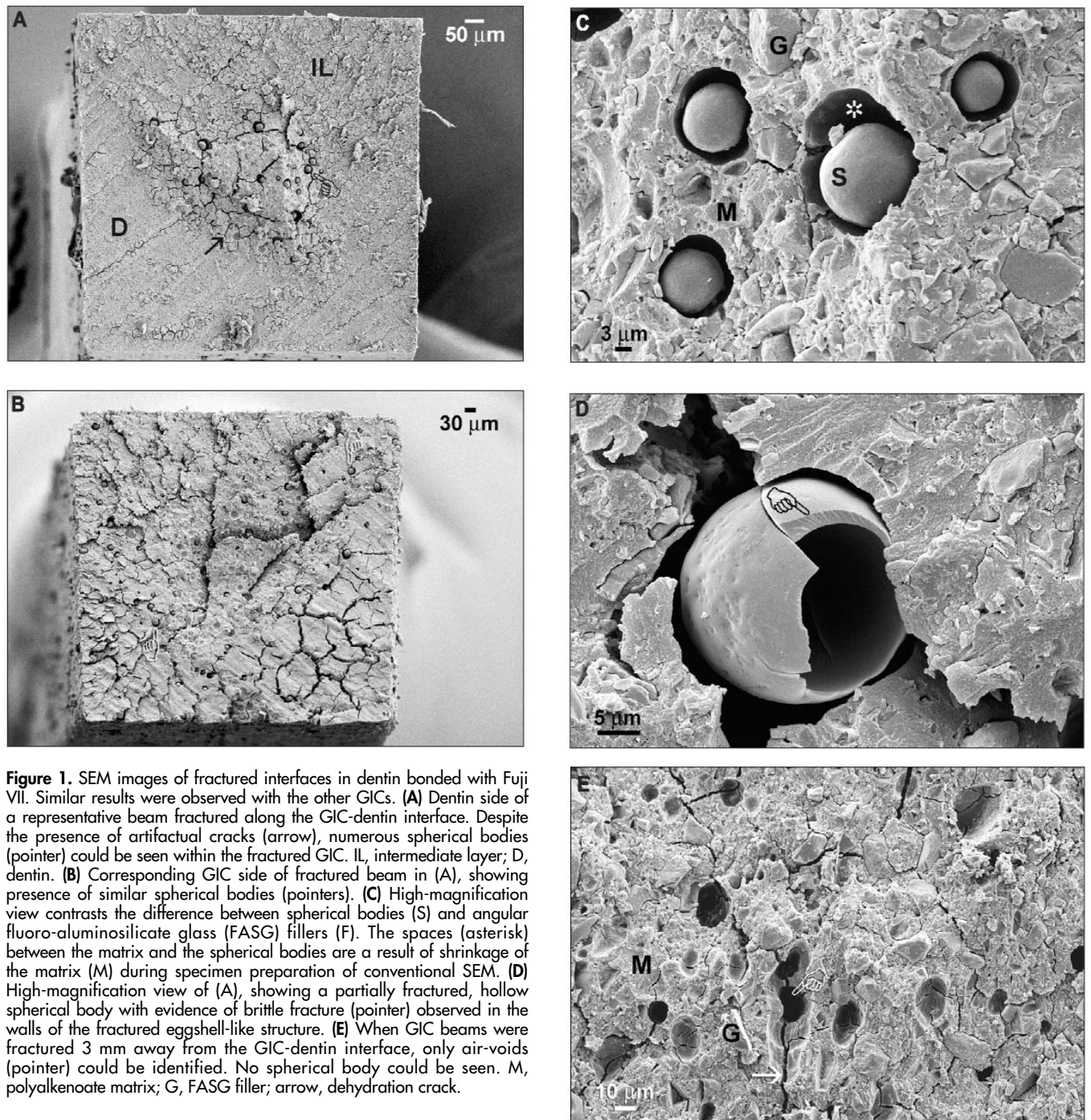


Figure 1. SEM images of fractured interfaces in dentin bonded with Fuji VII. Similar results were observed with the other GICs. (A) Dentin side of a representative beam fractured along the GIC-dentin interface. Despite the presence of artifactual cracks (arrow), numerous spherical bodies (pointer) could be seen within the fractured GIC. IL, intermediate layer; D, dentin. (B) Corresponding GIC side of fractured beam in (A), showing presence of similar spherical bodies (pointers). (C) High-magnification view contrasts the difference between spherical bodies (S) and angular fluoro-aluminosilicate glass (FASG) fillers (F). The spaces (asterisk) between the matrix (M) and the spherical bodies are a result of shrinkage of the matrix (M) during specimen preparation of conventional SEM. (D) High-magnification view of (A), showing a partially fractured, hollow spherical body with evidence of brittle fracture (pointer) observed in the walls of the fractured eggshell-like structure. (E) When GIC beams were fractured 3 mm away from the GIC-dentin interface, only air-voids (pointer) could be identified. No spherical body could be seen. M, polyalkenoate matrix; G, FASG filler; arrow, dehydration crack.

A siliceous hydrogel layer could also be identified along the periphery of the FASG fillers (Fig. 4B). Spherical bodies that were occasionally sectioned were found to be hollow, completely devoid of FASG fillers, and with an ultrastructural structure that resembled that of the adjacent polyalkenoate matrix phase more than the siliceous hydrogel layers of the FASG fillers (Fig. 4C).

DISCUSSION

The spherical bodies were consistently identified in all 6 autocured GICs during ultrastructural examination of the bonded

interfaces by SEM, FE-ESEM, and TEM. The presence of these spherical bodies in the matrices of GICs at the GIC-dentin interface, but their absence 0.5 mm from the dentin, suggests that they are formed from water that slowly permeates from dentin into the GIC matrix. The presence of moisture in the specimen chamber of FE-ESEM allows for examination of GIC in a hydrated status. The close association of these spherical bodies with the GIC-dentin interface under FE-ESEM examination suggested that the mechanism of spherical body formation depends on the permeability of the GIC-dentin interface and the availability of water from the underlying moist dentin.

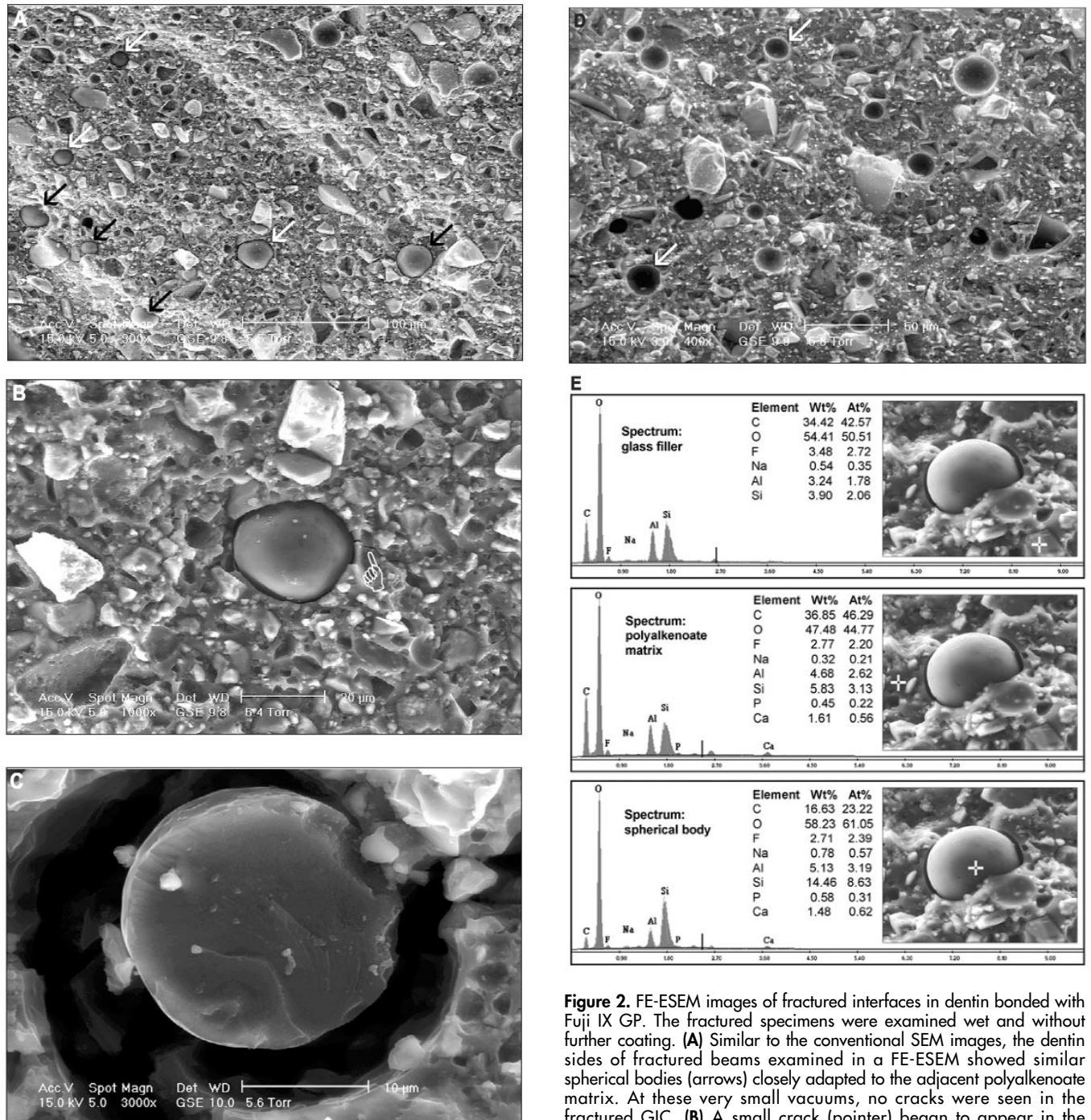


Figure 2. FE-ESEM images of fractured interfaces in dentin bonded with Fuji IX GP. The fractured specimens were examined wet and without further coating. (A) Similar to the conventional SEM images, the dentin sides of fractured beams examined in a FE-ESEM showed similar spherical bodies (arrows) closely adapted to the adjacent polyalkenoate matrix. At these very small vacuums, no cracks were seen in the fractured GIC. (B) A small vacuum (pointer) began to appear in the polyalkenoate matrix, adjacent to a spherical body, as the vapor pressure was reduced to 5.4 Torr. (C) Shrinkage of the polyalkenoate matrix resulted in irreversible separation of the latter from the spherical bodies, even after the vapor pressure was returned to 5.6 Torr. A fractured spherical body revealed the presence of a solid core that was probably due to the retention of water within the eggshell-like structure. (D) Fractured unbonded Fuji IX GP (control) showed the absence of spherical bodies within the polyalkenoate matrix. Only air-voids (arrows) could be observed. (E) EDX analysis of Fuji IX GP-bonded dentin that was fractured along the GIC-dentin interface and examined with FE-ESEM. The elemental composition included Ca and P within the polyalkenoate matrix and Si in the spherical bodies and FASG fillers.

pressure was reduced to 5.4 Torr. (C) Shrinkage of the polyalkenoate matrix resulted in irreversible separation of the latter from the spherical bodies, even after the vapor pressure was returned to 5.6 Torr. A fractured spherical body revealed the presence of a solid core that was probably due to the retention of water within the eggshell-like structure. (D) Fractured unbonded Fuji IX GP (control) showed the absence of spherical bodies within the polyalkenoate matrix. Only air-voids (arrows) could be observed. (E) EDX analysis of Fuji IX GP-bonded dentin that was fractured along the GIC-dentin interface and examined with FE-ESEM. The elemental composition included Ca and P within the polyalkenoate matrix and Si in the spherical bodies and FASG fillers.

EDX and TEM results further confirmed that the shells of these spherical bodies were not simply siliceous hydrogel layers of the FASG fillers, since the latter contained distinct fluoride-rich, electron-dense, "seed-like" phases that are characteristic of the original glass composition (Barry *et al.*,

1979; Tay *et al.*, 2001b). Rather, the eggshell-like structure represents a distinct Si-rich phase that has a composition slightly different from that of the original polyalkenoate matrix. The Si-rich phase is probably formed as a result of water diffusion across the bonded interface, initiating the

delayed GI reaction that occurred during the maturation phase of GIC. Since permeation of water into GIC is a diffusion-controlled process, we speculate that a longer storage time will allow more spherical bodies to form. The presence of this secondary phase resembles the silica phase that was observed following the aging of GICs (Wasson and Nicholson, 1993; Matsuya *et al.*, 1996). Undeniably, the EDX used during FE-ESEM examination has a relatively large depth of compositional analysis that may affect the accuracy of our results. However, recent examination of elemental compositions of spherical bodies by TEM/EDX analysis resulted in similar conclusions (Tay, unpublished results).

The difference between the hollow appearance of the spherical bodies, as observed with SEM and TEM, and their solid appearance, under FE-ESEM, may be attributed to the presence of a pool of water within the eggshell-like structure when specimens were examined by the latter technique. When the specimens were examined by conventional SEM, the water probably evaporated from the fractured shells, revealing the original eggshell-like characteristics.

Since the GICs were protected with resin-coatings in the present study, water for the additional GIC reaction could be provided only by the underlying moist dentin. Such a phenomenon parallels what has been recently reported for single-step, self-etch dentin adhesives (Tay *et al.*, 2002), in which water can diffuse from moist dentin through the adhesive layer to form water droplets along the adhesive-composite interface, with the adhesive layer acting as a semi-permeable membrane. Since an intermediate layer (Tanumiharja *et al.*, 2001) is present between dentin and GIC (Fig. 4A), we hypothesize that a similar osmotic gradient may exist in the ion-rich polyalkenoate matrix that causes permeation of water across the GIC-dentin interface and initiated the additional GI reaction. Although such a hypothesis awaits confirmation, it provides a rationale for why only air-voids were observed when GIC-bonded dentin specimens were fractured at sites farther from the bonded interfaces. It also provides a reasonable explanation for the observed water permeation from dentin into GICs (Watson *et al.*, 1998) during dynamic imaging of GIC-bonded dentin.

The additional Si-rich phase represented by these spherical bodies probably played an important role in strengthening GIC along the bonded interface. Leiskar *et al.* (2003) reported a continuous increase in shear punch strength for up to 2 wks when Fuji IX GP, that was not initially protected by a resin coating, was exposed to water. Similar results were reported by Miyazaki *et al.* (1996). The clinical implication is that bonded GICs will continue to draw water from the underlying moist dentin for additional acid-base reaction—a process that does not occur in GIC-bonded enamel, due to its lower water content (ten Bosch *et al.* 2000). The clinical disadvantage is that the GIC may draw water from dentin fast enough to cause the occasional post-operative sensitivity (Christensen, 1990) that is associated with their use.

In conclusion, in the absence of water-sorption from external sources, the existence of a distinct Si-rich phase within the air-voids of GIC-bonded dentin is probably caused by the permeation of water across the GIC-dentin interface, as previously reported by Watson *et al.* (1998). Since similar water movement across bonded resin-modified

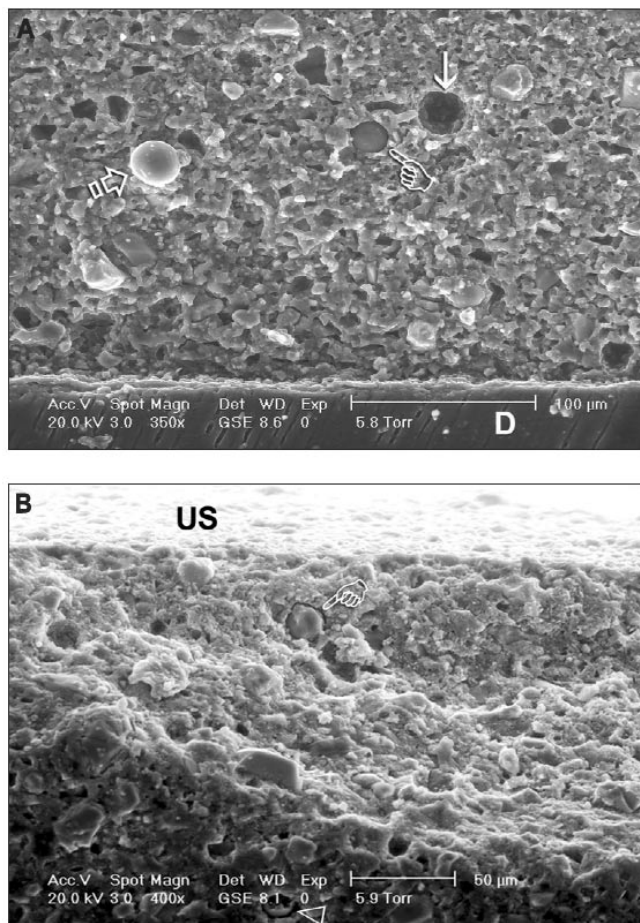


Figure 3. FE-ESEM images of polished, intact interfaces that were bonded with Fuji VII. The polished surfaces were briefly etched with phosphoric acid to remove the smear layer and to bring the interfaces into relief. (A) Representative example from specimens with the exposed GIC surface sealed with resin immediately after placement. A spherical body, still embedded within the polyalkenoate matrix, was seen 150 μm away from the bonded dentin (D). Another spherical body (open arrow) was probably dislodged from an adjacent air-void (arrow). No spherical bodies were observed from either the bonded enamel or along the exposed GIC surface (not shown). (B) Representative example from specimens in which the exposed GIC surface was not sealed and exposed to water for 10 min prior to storage at 100% relative humidity. The surface of the GIC was partially fractured during sectioning, exposing a spherical body (pointer) that was about 30 μm away from the unsealed GIC surface (US). Another partially intact spherical body (open arrowhead) could be seen further down the polished surface at about 180 μm from the unsealed GIC surface. Only air-voids could be identified further down the polished surface.

GICs has resulted in the formation of an amorphous "absorption layer" (Sidhu and Watson, 1998; Sidhu *et al.*, 1999, 2002), further research should be performed to examine if similar spherical bodies could be seen in this class of restorative material.

ACKNOWLEDGMENTS

This study was based on the work partially performed by Cynthia Yiu for the fulfillment of the degree of Doctor of Philosophy, the University of Hong Kong. We thank W.S. Lee

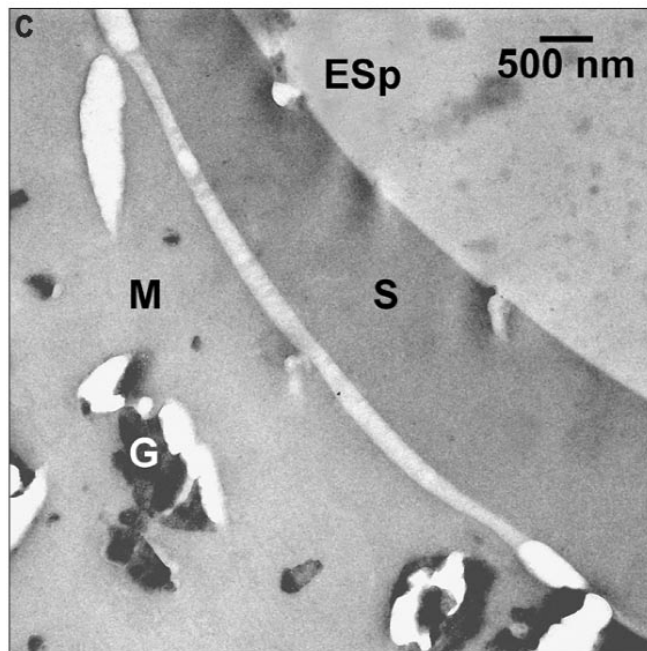
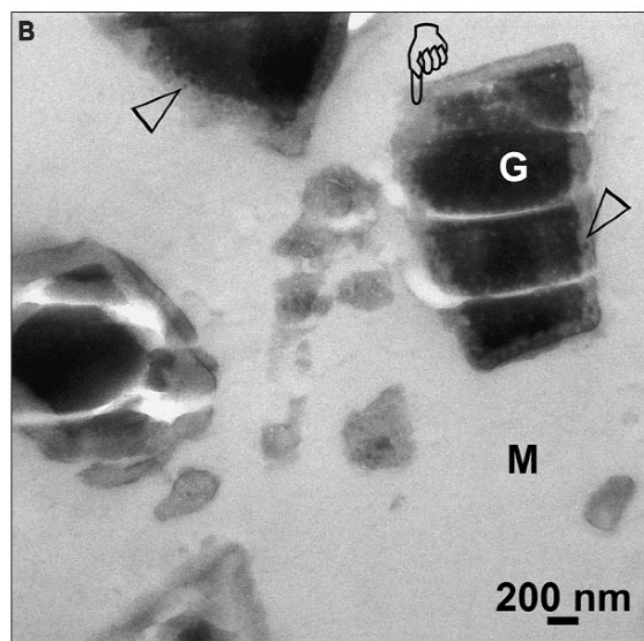
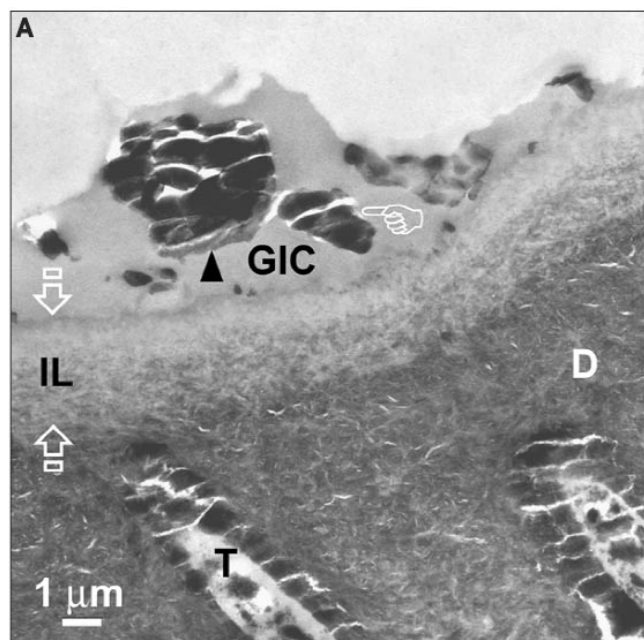


Figure 4. TEM images of regions that were close to the GIC-dentin interfaces. **(A)** The GIC-dentin interface in ChemFlex showed the presence of a 3- μm -thick, partially demineralized, intermediate layer (IL; between open arrows) between the dentin (D) and the fractured GIC (GIC). The originally intact GIC was fractured during ultramicrotomy. FASG fillers (pointer) with a peripheral siliceous hydrogel layer (arrowhead) could be seen within the remnant GIC. T, dentinal tubule. **(B)** A high-magnification view of the polyalkenoate matrix (M) from a dentin specimen that was bonded with the experimental GIC K-136 (Dentsply DeTrey). Siliceous hydrogel layers (pointer) could be seen along the periphery of the FASG fillers (G). Within the siliceous hydrogel layer, numerous "seed-like", electron-dense fluoride-rich phases could be observed (open arrows). **(C)** A high-magnification view of the polyalkenoate matrix that was sectioned close to the GIC-dentin interface in ChemFlex. A portion of the wall of a hollow spherical body (S) could be seen. This wall resembled the adjacent polyalkenoate matrix (M) in ultrastructural appearance, but was separated from the latter. ESp, empty space that was occupied by the Formvar-coated copper grid.

of the Electron Microscopy Unit, the University of Hong Kong, for technical assistance. The glass-ionomer cements examined were generous gifts from the respective manufacturers. This study was supported, in part, by grant 20003755/90800/08004/400/01, the Faculty of Dentistry, the University of Hong Kong, and by grant DE014911 from the NIDCR, USA. The authors are grateful to Zinnia Pang and Michelle Barnes for secretarial support.

REFERENCES

- Barry TI, Clinton DJ, Wilson AD (1979). The structure of a glass-ionomer cement and its relationship to the setting process. *J Dent Res* 58:1072-1079.
- Christensen GJ (1990). Glass ionomer as a luting material. *J Am Dent Assoc* 120:59-62.
- Cowan AJ, Wilson NH, Wilson MA, Watts DC (1996). The application of ESEM in dental materials research. *J Dent* 24:375-377.
- Ferrari M, Davidson CL (1997). Interdiffusion of a traditional glass ionomer cement into conditioned dentin. *Am J Dent* 10:295-297.
- Geiger SB, Weiner S (1993). Fluoridated carbonatoapatite in the intermediate layer between glass ionomer and dentin. *Dent Mater* 9:33-36.
- Glasspoole EA, Erickson RL, Davidson CL (2002). Effect of surface treatments on the bond strength of glass ionomers to enamel. *Dent Mater* 8:454-462.
- Hatton PV, Brook IM (1992). Characterization of the ultrastructure of glass-ionomer (polyalkenoate) cement. *Br Dent J* 173:275-277.
- Kerby RE, Knobloch L (1992). Strength characteristics of glass-ionomer cements. *Oper Dent* 17:172-174.
- Leirskar J, Nordbø H, Mount GJ, Ngo H (2003). The influence of resin

- coating on the shear punch strength of a high strength auto-cure glass ionomer. *Dent Mater* 19:87-91.
- Maeda T, Mukaeda K, Shimohira T, Katsuyama S (1999). Ion distribution in matrix parts of glass-polyalkenoate cement by SIMS. *J Dent Res* 78:86-90.
- Matsuya S, Maeda T, Ohta M (1996). IR and NMR analyses of hardening and maturation of glass-ionomer cement. *J Dent Res* 75:1920-1927.
- Miyazaki M, Moore BK, Onose H (1996). Effect of surface coatings on flexural properties of glass ionomers. *Eur J Oral Sci* 104:600-604.
- Nassan MA, Watson TF (1998). Conventional glass ionomers as posterior restorations. A status report for the *American Journal of Dentistry*. *Am J Dent* 11:36-45.
- Ngo H, Mount GJ, Peters MC (1997). A study of glass-ionomer cement and its interface with enamel and dentin using a low-temperature, high-resolution scanning electron microscopic technique. *Quintessence Int* 28:63-69.
- Nicholson JW (1998). Chemistry of glass-ionomer cements: a review. *Biomaterials* 19:485-494.
- Sennou HE, Lebugle AA, Grégoire GL (1999). X-ray photoelectron spectroscopy study of the dentin-glass ionomer cement interface. *Dent Mater* 15:229-237.
- Sidhu SK, Watson TF (1998). Interfacial characteristics of resin-modified glass-ionomer materials: a study on fluid permeability using confocal fluorescence microscopy. *J Dent Res* 77:1749-1759.
- Sidhu SK, Sherriff M, Watson TF (1999). Failure of resin-modified glass-ionomer subjected to shear loading. *J Dent* 27:373-381.
- Sidhu SK, Pilecki P, Cheng PC, Watson TF (2002). The morphology and stability of resin-modified glass-ionomer adhesive at the dentin/resin-based composite interface. *Am J Dent* 15:129-136.
- Tanumiharja M, Burrow MF, Cimmino A, Tyas MJ (2001). The evaluation of four conditioners for glass ionomer cements using field-emission scanning electron microscopy. *J Dent* 29:131-138.
- Tay FR, Smales RJ, Ngo H, Wei SH, Pashley DH (2001a). Effect of different conditioning protocols on adhesion of a GIC to dentin. *J Adhes Dent* 3:153-167.
- Tay FR, Pashley EL, Huang C, Hashimoto M, Sano H, Smales RJ, et al. (2001b). The glass ionomer phase in resin-based restorative materials. *J Dent Res* 80:1808-1812.
- Tay FR, Pashley DH, Suh BI, Carvalho RM, Itthagarun A (2002). Single-step adhesives are permeable membranes. *J Dent* 30:371-382.
- ten Bosch JJ, Fennis-le Y, Verdonschot EH (2000). Time-dependent decrease and seasonal variation of the porosity of recently erupted sound dental enamel *in vivo*. *J Dent Res* 79:1556-1559.
- Wasson EA, Nicholson JW (1993). New aspects of the setting of glass-ionomer cements. *J Dent Res* 72:481-483.
- Watson TF, Billington RW, Williams JA (1991). The interfacial region of the tooth/glass-ionomer restoration: a confocal optical microscope study. *Am J Dent* 4:303-310.
- Watson TF, Pagliari D, Sidhu SK, Nassan MA (1998). Confocal microscope observation of structural changes in glass-ionomer cements and tooth interfaces. *Biomaterials* 19:581-588.
- Yip HK, Tay FR, Ngo HC, Smales RJ, Pashley DH (2001). Bonding of contemporary glass ionomer cements to dentin. *Dent Mater* 17:456-470.